Luminescence flashes induced by microwave radiation in undoped GaAs quantum wells

I. Baskin, B. M. Ashkinadze, and E. Cohen
Solid State Institute, Technion-Israel Institute of Technology, Haifa 32000, Israel

L. N. Pfeiffer
Department of Electrical Engineering, Princeton University, Princeton, New Jersey 08544, USA
(Received 16 March 2009; published 26 May 2009)

Bright flashes of exciton emission are observed in photoexcited, undoped GaAs/AlGaAs quantum wells under pulsed microwave (36 GHz) irradiation. The flash intensity is in the range of 10–100 times the steady-state photoluminescence intensity with a decay time of $(1-10)\times 10^{-8}$ s (depending on the applied microwave power and photoexcitation). These observations indicate a reservoir of long-lived carriers that is formed at low temperature due to localization of photogenerated electrons and holes at spatially separated shallow traps. Microwave-heated electrons activate the localized carriers into free states by means of avalanche impact ionization. This gives rise to rapid exciton formation with subsequent luminescence flash. A detailed model based on the coupled rate equations for free electrons, excitons and localized electrons (holes) is presented.

DOI: 10.1103/PhysRevB.79.195325 PACS number(s): 73.50.Mx, 78.70.Gq

I. INTRODUCTION

In bulk semiconductors, photoexcited electrons and holes can be accumulated at low temperatures in long-lived bound states, and this gives rise to several effects such as stimulated impurity photoconductivity,[1] persistent photoconductivity,[2,3] and enhancement of the optical nonlinearity for photon energies below the band gap.[4]

A long lifetime of photoexcited electron-hole pairs, especially in direct band-gap semiconductors, is evidence for spatial separation of electrons and holes. It is an inherent property of compound semiconductors (e.g., GaAs and AlGaAs) where electrons and holes are localized at the states below the bandgap by various imperfections.[3] The activation of these localized carriers can lead to modulation of both conductivity[2,3] and photoluminescence (PL).[5]

In undoped quantum well (QW) heterostructures, well-width fluctuations and interface imperfections can provide additional shallow localizing sites for spatially separated long-lived electrons and holes. These states play a crucial role in the low-temperature dynamics of the excitons, giving rise to prolonged PL intensity decay[6] and to PL spectral variations with increased photoexcitation intensity[7,8] or electron temperature.[9,10] Spin dynamics in QWs is also affected by these long-lived carriers.[11] Photogenerated *e-h* pairs can be spatially separated either by an electric field application along the growth direction[12] or by a strong piezoelectric field accompanying surface acoustic waves.[13] The subsequent activation of the spatially separated electrons and holes gives rise to a delayed light flash that can be used for storage of light.[14]

Here we report on bright flashes of exciton PL that are induced by pulsed microwave (mw) radiation in undoped GaAs/AlGaAs QWs at low temperatures. Excitons do not interact directly with the mw electric field since they are neutral entities. However, mw radiation heats up free electrons that subsequently activate localized carriers into delocalized states. Free electrons and holes (*e-h*) then form excitons, giving rise to the observed intense PL flashes. A model describing the transient excitonic PL response to short mw pulses is developed. It is based on *e-h* dynamics, namely, electron localization, impact ionization, and exciton formation.

The paper is laid out as follows. Section II details the studied samples and experimental methods. In Sec. III, the experimental results for the time-resolved mw-induced PL changes are presented. The origin of the mw-induced flashes of exciton emission is discussed in Sec. IV. Conclusions are presented in Sec. V.

II. EXPERIMENTAL DETAILS

The undoped $GaAs/Al_{0.3}Ga_{0.7}As$ multiple QW samples used in our experiments were grown by molecular beam epitaxy (MBE) on a (001)-GaAs substrates. Each structure consists of 10–50 periods of GaAs/AlGaAs quantum wells separated by undoped $Al_{0.3}Ga_{0.7}As$ barriers. Each multiple QW heterostructure differs in the QW and barrier layer widths that vary in the range of 5–20 and 10–80 nm, respectively.

The sample was mounted inside a short-circuited 8 mm waveguide, at the maximum of the mw electric field, which was in the QW plane. It was illuminated (through a small hole in the waveguide) by a laser diode with light intensity of $I_L < 100$ mW/cm^2 at a photon energy of $E_L = 1.56$ eV (below the barrier band gap). In some experiments the laser beam was pulse modulated with an acousto-optic modulator (pulse width of 5 μs). Mw radiation at 36 GHz ($\approx$0.17 meV) was supplied by a Gunn diode. The incident mw power P_{mw} was varied in the range of 0.1–20 mW and it was modulated with a high-speed *p-i-n* switch. The mw-pulse duration and modulation frequency were varied in the ranges of 40–200 ns and $F_{rep} = (5-0.005)$ MHz, respectively.

The PL was spectrally analyzed by a spectrometer with resolution of 0.1 meV and the signal was detected by a cooled photomultiplier having a response time of $\sim$2 ns. The time-resolved PL study was performed either with a gated photon counter or by using the time-correlated single-photon counting technique. Mw and light pulse have rise (fall) time of 5 and 50 ns, respectively. The experiments were

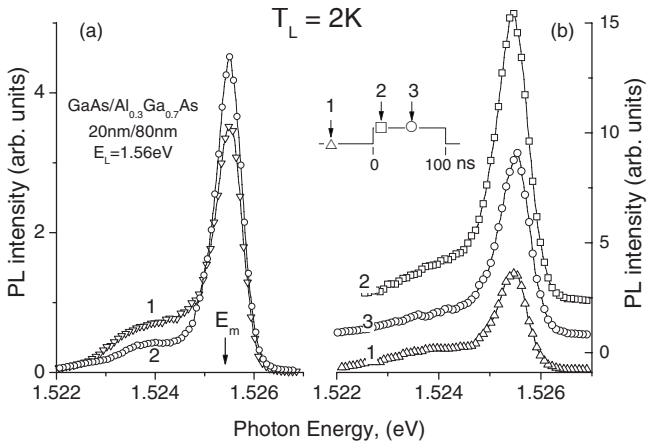

FIG. 1. PL spectra of an undoped 20-nm-wide multiple QW sample. Cw excitation at $E_L=1.56$ eV and $I_L=5$ mW/cm^2. (a) Curve 1 – $P_{mw}=0$, curve 2–cw $P_{mw}=10$ mW. (b) Time-resolved PL spectra under pulsed mw irradiation, measured at −100, +5, and +20 ns delay times (curves 1–3, respectively) and $P_{mw}=10$ mW. The curves are vertically shifted for clarity. The inset displays the 100 ns mw-pulse waveform and the symbols indicate when the PL spectra were measured.

done at $T_L=2$ K with the sample immersed in liquid He.

III. RESULTS

All the studied QWs show similar mw-induced PL modulation effects. Here we present the results of a multiple 20-nm-wide QW (10 periods) sample. The PL spectra obtained in the absence and under cw mw irradiation are shown in Fig. 1(a), curves 1 and 2, respectively. The strongest PL line in the spectra is due to free $(1e:1hh)1s$ excitons (FE) while the low energy, wide PL band results from localized excitons.[7,9]

Cw mw irradiation causes a PL spectral intensity redistribution between the bands.[9] In the studied high quality QWs, the increased FE PL intensity is small (<20%) and the spectrally integrated intensity changes only slightly (~3% even for highest incident mw power, $P_{mw}<20$ mW).

Contrary to the moderate PL changes observed under cw mw irradiation, a strong transient PL modulation is observed under irradiation with short mw pulses. Figure 1(b) shows several time-resolved PL spectra obtained at various delay times relative to the leading edge of a 100 ns duration mw pulse (as illustrated in the inset). These spectra were measured with a 5 ns time resolution. A ~3-fold intensity enhancement of the entire PL spectrum is observed at the beginning of mw pulse, namely, at a 5 ns delay [curve 2 in Fig. 1(b)]. At larger delay times, the PL intensity decreases (curve 3) but it is still stronger than that observed under cw mw. The PL observed at delay times of 70–100 ns is the same as that observed under cw mw [Fig. 1(a)]. Curve 1 in Fig. 1(b) shows the time-resolved spectrum measured between the mw pulses (delay time of −100 ns or $\geqslant$+100 ns), and this spectrum is similar to cw PL observed at $P_{mw}=0$ [curve 1 in Fig. 1(a)].

A remarkable time evolution of mw-induced PL changes was found by studying the PL intensity transients shown

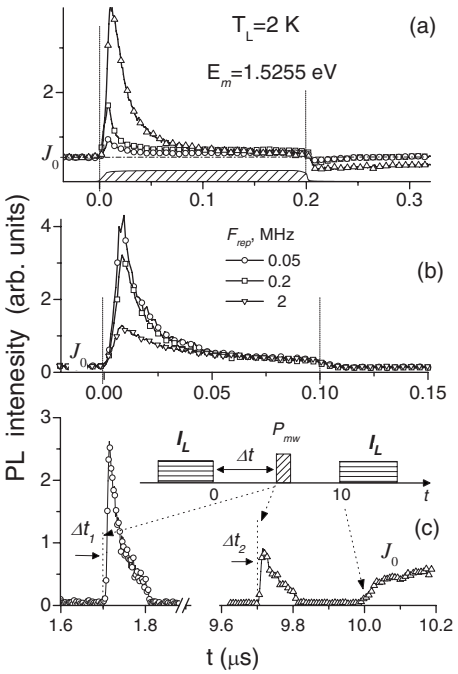

FIG. 2. Transient exciton PL intensity induced by a short mw pulse. J_0 marks the steady-state PL intensity at $P_{mw}=0$. (a) Transients measured at the following I_L(mW/cm^2) and P_{mw}(mW) values: (2, 20)—triangles; (10, 20)—squares; (10, 2)—circles. (The signals at $I_L=10$ mW/cm^{2}are divided by five for comparison with the first transient.) The mw-pulse waveform is shown by the hatched area. (b) Transients obtained at several repetition rates of 0.1 μs mw pulses. $I_L=0.2$ mW/cm^2, $P_{mw}=10$ mW. (c) Photoluminescence flashes triggered by 0.1 μs-mw pulses applied with time delay after the laser-pulse termination, $\Delta t_1=1.7$ μs (circles) and $\Delta t_2=9.7$ μs (triangles). $I_L=20$ mW/cm^2, $P_{mw}=10$ mW. The inset shows photoexcitation and mw-pulses timing (with $\Delta t=\Delta t_1$, Δt_2).

in Fig. 2. These transients were obtained with a time resolution of ~2 ns at a monitored photon energy $E_m=1.5255$ eV [at the FE PL peak, marked by an arrow in Fig. 1(a)].

Under high P_{mw} (20 mW) and low photoexcitation ($I_L=2$ mW/cm^2), a strong PL intensity flash appears at the leading edge of the mw pulse [Fig. 2(a), triangle symbols]. The rise time of the flash is very short (<5 ns) while its decay time varies with P_{mw} in the range of 15–100 ns. As the laser intensity I_L increases, the flash amplitude decreases as shown by the square symbols transient in Fig. 2(a). Under low P_{mw}, the PL transient (circles) approximately follows the mw pulse waveform: a weak spike can still be seen at the leading edge and the PL intensity under mw pulse increases by ~20%. As the mw pulse is turned off, the PL signal drops slightly below its steady-state value and then it recovers with a characteristic time of ~200 ns.

Under a very low photoexcitation intensity, the flash amplitude reaches a value 100-fold that of the steady-state PL intensity, J_0. Figure 2(b) shows PL transients at $I_L=0.2$ mW/cm^2 obtained with 100 ns mw pulses of various repetition rate, F_{rep}. The PL flash amplitude is nearly independent of F_{rep} below 0.1 MHz and then it strongly decreases

with F_{rep}. This gives evidence for a long relaxation time (at least of 10 μs) of mw-induced processes in undoped QW.

Another finding is the mw-induced PL flashes observed as the mw pulses are applied between the photoexcitation pulses [inset of Fig. 2(c)]. Figure 2(c) displays the PL intensity transients obtained under pulsed light excitation (I_L), and it shows that the 100 ns mw pulses induce sharp FE intensity flashes during the light-off intervals. The flash intensity decreases with increasing the delay, Δt, between the I_L and P_{mw} pulses. This is demonstrated by traces obtained for $\Delta t = 1.7$ and 9.7 μs (circles and triangles, respectively). From this we conclude that the characteristic lifetime of the "dark photoexcited states" that are mw-activated and produce a PL flash, is ~ 10 μs. We note that the PL flash amplitudes exceed the steady-state PL signal J_0, which follows the light pulse waveform as seen in Fig. 2(c).

IV. MODEL AND DISCUSSION

The observed mw-induced PL changes are caused by free electrons that are heated by the mw electric field $\mathcal{E}$ so that the effective electron temperature T_e rises. The simplest T_e estimate can be obtained from the balance of the power that is gained and lost by the free electron: $e\mu\mathcal{E}^2 = (T_e - T_L)/\tau_\varepsilon$.[15] Here, μ and τ_ε are the electron mobility for an undoped QW [$\sim 1\times 10^5$ cm^2/V s (Ref. 16)] and the energy relaxation time [~ 0.5 ns (Ref. 15)]. At $P_{mw}=20$ mW, the mw electric field in the waveguide $\mathcal{E}$ is of ~ 15 V/cm. Then, the maximal estimated T_e^{max} is of ~ 15 K.

Electrons, heated by the mw, transfer the gained energy to localized excitons and electrons and delocalize them. Therefore, the intensity of the PL band due to localized excitons decreases while the FE PL intensity slightly increases. Under cw mw irradiation [see Fig. 1(a)], only weak mw-induced PL intensity changes are observed in high quality undoped QWs.[9] This is in contrast to bulk semiconductors and to QWs of a lesser quality where intense low-energy PL bands due to bound excitons are observed [e.g., in mixed type I-type II GaAs/AlAs QWs (Ref. 17)]. In these cases, electron heating generally causes quenching of the total excitonic PL since delocalized excitons (electrons) efficiently recombine nonradiatively.[18,19]

It should be noticed that no FE line broadening is observed in QWs studied here. This means that hot electrons do not affect the FE energy distribution. From this we conclude that the energy transfer from hot electrons (of low density) to free excitons is ineffective.

The intense FE PL flash observed at the leading edge of mw pulse as well as the mw-induced flash in the light-off interval give unambiguous evidence that photoexcited electrons and holes are effectively trapped at localized, long-lived "dark states" and form a reservoir containing a large amount of localized carriers. These localized electrons and holes are spatially separated and their recombination occurs very slowly as detected by the mw-induced PL flashes in Fig. 2(c).

Under mw irradiation, the hot electrons cause avalanche impact ionization of the localized electrons (holes) and activate them into their respective bands. At the mw-pulse leading edge, the free electron and hole densities rapidly increase and a high exciton density N_x is promptly generated, giving rise to the PL flash. As soon as the reservoir of localized carriers empties, N_x decreases since the exciton recombination time τ_x is short (~ 2 ns).[18,20] Then, the photoexcited system relaxes into a new steady state that depends on photogeneration rate and P_{mw}. As the mw pulse is turned off, the FE PL intensity drops below its steady-state value J_0 [Fig. 2(a), triangle symbols curve] and then, it slowly recovers to J_0. This is a result of the competing processes of exciton formation and slow recharging of shallow traps.

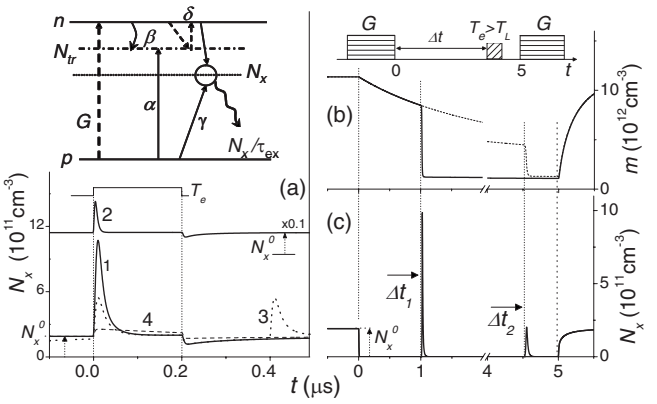

FIG. 3. Numerical simulated exciton density transient induced by a hot-electron (T_e) pulse at $T_L=2$ K. Top left panel schematically shows the processes included in the model. (a) The transients induced by T_e pulses of 0.2 μs duration under cw light excitation ($N_{tr}=2\times 10^{13}$ cm^{-3}). Curve 1: $G=10^{20}$ cm^{-3} s^{-1}, $T_e=10$ K, and $F_{rep}=0.4$ MHz. Curves 2–4 are calculated as one of parameters varies: $G=10^{21}$ cm^{-3} s^{-1}, $F_{rep}=2.5$ MHz, and $T_e=3$ K, respectively. Curve 2 is multiplied by 0.1 and vertically shifted for clarity. N_x^0 is the steady-state exciton density. (b) Trapped electron and (c) exciton density transients under pulsed light and mw excitation (pulse timing is displayed in the inset). T_e pulses of 0.2 μs are applied with delays of $\Delta t_1=1$ μs (solid) and $\Delta t_2=4.5$ μs (dashed) between G pulses (in the interval of 5 μs). $G=1\times 10^{20}$ cm^{-3} s^{-1}, $N_{tr}=2\times 10^{13}$ cm^{-3}, $F_{rep}=0.1$ MHz, and $T_e=20$ K.

These qualitative explanations are supported by the model that takes into account the physical processes schematically depicted in Fig. 3. The corresponding rate equations for the densities of free and localized electrons (n and m, respectively), excitons (N_x) and holes (p) are given by Eqs. (1)–(3). Equation (4) results of neutrality of the system. N_{tr} is the shallow electron trap density,

$$\frac{dn}{dt} = G - \gamma np - \beta(N_{tr} - m) + \delta nm, \tag{1}$$

$$\frac{dm}{dt} = \beta(N_{tr} - m) - \delta nm - \alpha pm, \tag{2}$$

$$\frac{dN_x}{dt} = \gamma np - N_x/\tau_{ex}, \tag{3}$$

$$p = m + n, \tag{4}$$

where G is the free-electron-hole pair generation rate by interband photoexcitation, γnp is the e-h bimolecular binding rate into free exciton, and $\beta(N_{\rm tr}-m)$ and δnm describe capture of electrons by empty traps and impact ionization of localized electrons by free electrons. The nonradiative recombination rate of the localized electrons is given by αpm. Since all experiments are done at low temperature, all thermal ionization processes of excitons and traps are neglected. Also, the model does not account for free and localized exciton redistribution which is most pronounced in the cw mw experiments [see Fig. 1(a)].[9]

In general, the coefficients γ, β, and δ depend on T_e, which rises due to mw heating. We assume that hot electrons mainly affect the $\delta(T_e)$ dependence and neglect the weaker $\gamma(T_e)$ and $\beta(T_e)$ dependence. For a Maxwellian distribution of hot electrons, $\delta \propto \exp(-E_{\rm tr}/T_e)$, (Refs. 18 and 20) where $E_{\rm tr}$ is the trap binding energy. Thus, $\delta(T_e)$ is the only parameter that is altered under pulsed mw irradiation.

In the steady state, Eqs. (1)–(3) reduce to $G = N_x^0/\tau_{ex} + \alpha mp$, where the first term is the exciton recombination rate. For the high quality QWs, the nonradiative recombination rate, αmp is much lower than the radiative one and we neglect this term ($\alpha = 0$). Then, the steady-state solutions of Eqs. (1)–(4) are

$$m_0 = \beta N_{\rm tr}/(\beta + \delta), \tag{5}$$

$$n_0 = \frac{1}{2}\frac{\beta N_{\rm tr}}{\beta+\delta}\left[\sqrt{1+4\frac{G}{\gamma}\left(\frac{\beta+\delta}{\beta N_{\rm tr}}\right)^2}-1\right], \tag{6}$$

$$N_x^0 = G\tau_{ex}. \tag{7}$$

It follows from Eqs. (5)–(7) that the traps are fully occupied ($m_0 = N_{\rm tr}$) in the absence of mw irradiation ($\delta = 0$), and mw radiation causes a strong reduction of the localized electron density while the steady-state exciton density value is unaffected by mw (assuming $\alpha = 0$). The measured FE PL intensity (J) is proportional to N_x/τ_x.

However, an exciton density spike does occur in the transient mw-induced effect. At low photogeneration ($G/\gamma \ll N_{\rm tr}^2$), Eq. (6) gives $n_0 \approx \frac{G}{\gamma}\frac{\beta+\delta}{\beta N_{\rm tr}} \approx G/\gamma N_{\rm tr}$, and $n_0 \ll m_0 \approx N_{\rm tr} \approx p_0$ before the mw-pulse application ($\delta = 0$). After the mw pulse is turned on ($\delta \gg \gamma, \beta$), n strongly increases for a short time and approaches the value of $n \approx m_0$. Thus, an excitonic PL flash appears with an amplitude of $N_x \approx \gamma N_{\rm tr}^2 \tau_{ex} \gg G\tau_{ex} \approx N_x^0$ (see Eq. (3)). With increasing G, the ratio of densities of the electrons released from traps to the directly photogenerated ones, m_0/n_0 decreases, and thus, the PL flash amplitude is expected to decrease relative to the cw value, J_0.

The solution to Eqs. (1)–(4) was obtained by numerical simulations. The calculated transient traces shown in Figs. 3 contain the main PL transient features observed experimentally: (a) A sharp excitonic PL flash appears as T_e rises to 10 K [curve 1 in Fig. 3(a)]; (b) The ratio of the mw induced N_x to N_x^0 decreases with G [curve 2 in Fig. 3(a)]; (c) The exciton and trapped electron densities do not restore to their unperturbed values if the interval between the mw pulses is short enough [0.2 μs for curve 3 in the Fig. 3(a)]; (d) At $T_e = 3$ K, the exciton flash does not appear [curve 4 in Fig. 3(a)].

The transients in the case of both laser and mw-pulsed excitations [inset of Fig. 3(b)] are shown in Figs. 3(b) and 3(c). These $m(t)$ and $N_x(t)$ are calculated for $\Delta t = 1$ μs and 4.5 μs (solid and dashed curves, respectively). The simulation demonstrates a slow decay of $m(t)$ as the photoexcitation is turned off [Fig. 3(b)] and its sharp decrease in the leading mw-pulse edge with the simultaneous appearance of a N_x flash [Fig. 3(c)]. Thus, the simulated transients agree well with the experimental ones (Fig. 2) and this proves the validity of the developed model.

The following parameters were used in the numerical calculations: $G = \kappa I_L/E_L$, where κ is the absorption coefficient, $\kappa^{-1} \approx 1$ μm $\gg L$ (the QW width), $\tau_{ex} = 2$ ns; $\gamma = 7 \times 10^{-5}$ cm^3 s^{-1}, and $\delta_0 = 2 \times 10^{-4}$ cm^3 s^{-1}.[18,20] The localization sites were simulated by traps that have a binding energy of $E_{\rm tr} = 1$ meV and $N_{\rm tr} = 2 \times 10^{13}$ cm^{-3}.

The latter value was estimated from the experiment as follow: At $G_s \sim 3 \times 10^{20}$ cm^{-3} s^{-1}, the PL flash amplitude was about $\sim 2J_0 \approx 2G_s$ and it lasted for $\Delta t_{\rm flash} \cong 10^{-7}$ s [see Fig. 2(a)]. Then, the density of excitons in the mw-induced flash is $\Delta N_x \sim G_s \Delta t_{\rm flash} = 3 \times 10^{13}$ cm^{-3}. ΔN_x is of the order of Δn activated from the traps, thus $\Delta N_x \lesssim \Delta n \sim m_0$. We conclude (see Eqs. (5) and (6)) that $N_{\rm tr} \sim 3 \times 10^{13}$ cm^{-3} and the electron density in the absence of mw is $n_0 \sim G/\gamma N_{\rm tr} \simeq 10^{11}$ cm$^{-3} \ll m_0$. The presence of these traps can affect the exciton PL only at low G as $n_0 \ll m_0$.

The $E_{\rm tr}$ value is assumed to be ~ 1 meV because our experiments show that the free excitons (having binding energy of 6 meV) are not ionized under the mw power used. The localizing sites having $E_{\rm tr} \sim 1$ meV are probably due to either QW width fluctuations (interface roughness) or due to the conduction (valence)-band density of states tails in the forbidden band that are caused by residual disorder of the well material. The latter possibility is supported by the fact that QW structures of various widths 50–50 nm show similar mw-induced flashes.

The term αpm in Eq. (2) describes slow recombination of localized electrons after photoexcitation [see $m(t)$ dependence in Fig. 3(b)], and therefore the relaxation time $(\alpha p)^{-1}$ can be estimated from the reduced PL flash amplitude with increasing Δt [Fig. 2(c)]. This relaxation time is of 5 μs, and thus $\alpha = 1 \times 10^{-8}$ cm^3 s^{-1} ($p \sim N_{\rm tr}$, see Eq. (4)). The value of $\beta \approx 3 \times 10^{-5}$ cm^3 s^{-1} was obtained by fitting the simulated transient curves to the experimental PL kinetics.

The three-dimensional (bulk) parameters used in the calculations are applicable for the studied QWs of 20 nm width. The value of $N_{\rm tr} = 3 \times 10^{13}$ cm^{-3} corresponds to a two-dimensional trap density of $N_{\rm tr}^{2D} \approx 10^9$ cm^{-2} for the studied undoped, high quality QWs. The mw-induced carrier activation affects the excitonic PL at the low photogenerated free-electron density ($n_0 \ll N_{\rm tr}^{2D}$). However, the carriers activated from shallow traps do not contribute to the PL at higher photogeneration rates.

Traps of such density can also affect the properties of modulation-doped quantum wells (MDQWs) where the two-dimensional electron density is of 10^9–10^{10} cm^{-2}. It is,

therefore, reasonable to interpret the observed charged exciton (trion) PL line[8,21] as well as the conductivity behavior near the metal-isolator transition[22] as due to indigenous structural shallow traps in GaAs-based heterostructures.

V. CONCLUSION

We observed bright exciton PL flashes induced by pulsed mw irradiation in undoped GaAs QWs. The PL flash originates in an instant exciton generation caused by avalanche impact ionization of localized carriers. The activation of these long-lived "dark" electron and hole states into radiative (exciton) states can be considered as an upconversion process of the mw radiation into interband exciton emission.

The developed model accounts for impact ionization of localized electrons and subsequent formation of excitons and it leads to a valid simulation of the observed mw-induced PL flash transients. In addition, the density of localization sites and the effective life time of the trapped carriers are estimated. Our findings give unambiguous evidence that in undoped, high quality GaAs QWs, a reservoir containing a large density of localized carriers is created under interband photoexcitation. Plausible candidates for the localization traps in undoped QWs are interface fluctuations and inherent defects in the MBE-grown GaAs.

ACKNOWLEDGMENTS

The research at the Technion was supported by the Israeli Science Foundation (ISF), Jerusalem. B.M.A. acknowledges support by a grant under framework of the KAMEA Program.

[1] S. M. Ryvkin, *Photoelectric Effects in Semiconductors* (Consultants Bureau, New York, 1964), Chap. 10.
[2] M. K. Sheinkman and A. Ya. Shik, Fiz. Tekh. Poluprovodn. (S.-Peterburg) **10**, 209 (1976); Sov. Phys. Semicond. **10**, 128 (1976).
[3] H. J. Queisser and D. E. Theodorou, Phys. Rev. B **33**, 4027 (1986).
[4] N. Peyghambarian and S. W. Koch, in *"Semiconductor Nonlinear Materials," in Nonlinear Photonics*, edited by H. M. Gibbs, G. Khitrova, and N. Peyghambarian (Springer-Verlag, Berlin, 1990), Chap. 2.
[5] A. V. Akimov, V. V. Krivopalchuk, N. K. Poletaev, and V. G. Shofman, Fiz. Tekh. Poluprovodn. (S.-Peterburg) **27**, 314 (1993); Sov. Phys. Semicond. **27**, 171 (1993).
[6] I. Brener, M. Olszakier, E. Cohen, E. Ehrenfreund, Arza Ron, and L. Pfeiffer, Phys. Rev. B **46**, 7927 (1992).
[7] B. M. Ashkinadze, E. Linder, E. Cohen, Arza Ron and L. N. Pfeiffer, Phys. Rev. B **51**, 1938 (1995); B. M. Ashkinadze, E. Tsidilkovski, E. Linder, E. Cohen, Arza Ron and L. N. Pfeiffer, *ibid.* **54**, 8728 (1996).
[8] A. J. Shields, M. Pepper, D. A. Ritchie, M. Y. Simmons, and G. A. C. Jones, Phys. Rev. B **51**, 18049 (1995).
[9] B. M. Ashkinadze, E. Cohen, Arza Ron and L. Pfeiffer, Phys. Rev. B **47**, 10613 (1993).
[10] L. E. Golub, E. L. Ivchenko, and S. A. Tarasenko, Solid State Commun. **108**, 799 (1998).
[11] M. Syperek, D. R. Yakovlev, A. Greilich, J. Misiewicz, M. Bayer, D. Reuter, and A. D. Wieck, Phys. Rev. Lett. **99**, 187401 (2007).
[12] Y. Kan, M. Yamanishi, Y. Usami, and I. Suemune, IEEE J. Quantum Electron. **22**, 1837 (1986).
[13] C. Rocke, S. Zimmermann, A. Wixforth, J. P. Kotthaus, G. Böhm, and G. Weimann, Phys. Rev. Lett. **78**, 4099 (1997).
[14] J. P. Kotthaus, Science **286**, 2286 (1999); T. Lundstrom, W. Schoenfeld, H. Lee, P. M. Petroff *ibid.* **286**, 2312 (1999); J. Krauß, J. P. Kotthaus, A. Wixforth, M. Hanson, D. C. Driscoll, A. C. Gossard, Appl. Phys. Lett. **85**, 5830 (2004).
[15] K. Seeger, *Semiconductor Physics: An Introduction.*, 8th ed. (Springer, Berlin, 2002).
[16] M. Kozhevnikov, B. M. Ashkinadze, E. Cohen, Arza Ron and L. N. Pfeieffer, Superlattices Microstruct. **23**, 67 (1998).
[17] B. M. Ashkinadze, E. Linder, E. Cohen, L. N. Pfeiffer, Phys. Status Solidi C **1**, 514, (2004).
[18] B. M. Ashkinadze, A. G. Krasinskaya, and V. V. Bel'kov, Fiz. Tverd. Tela (Leningrad) **24**, 883 (1990); Sov. Phys. Solid State **25** 555 (1990).
[19] M. Godlewski, W. M. Chen, and B. Monemar, Crit. Rev. Solid State Mater. Sci. Sci. **19**, 241 (1994).
[20] J. Kundrotas, G. Valusis, A. Cėsna, A. Kundrotaitė, A. Dargys, A. Suziedėlis, J. Gradauskas, S. Asmontas, and K. Köhler, Phys. Rev. B **62**, 15871 (2000).
[21] G. Finkelstein, H. Shtrikman, and I. Bar-Joseph, Phys. Rev. Lett. **74**, 976 (1995).
[22] M. Yamaguchi, S. Nomura, T. Maruyama, S. Miyashita, Y. Hirayama, H. Tamura, and T. Akazaki, Phys. Rev. Lett. **101**, 207401 (2008).